

SPOT THE DIFFERENCES: THE X-RAY SPECTRUM OF SU AUR COMPARED TO TW HYA

K. Smith¹, M. Audard², M. Güdel³, S. Skinner⁴, and R. Pallavicini⁵

¹Max-Planck-Institut für Radioastronomie, Auf dem Hügel 69, D-53121 Bonn, Germany,

²Columbia Astrophysics Laboratory, Columbia University, Mail Code 5247, 550 West 120th Street, New York, NY 10027, USA

³Paul Scherrer Institute, Villigen & Würenlingen, 5232 Villigen PSI, Switzerland

⁴Center for Astrophysics and Space Astronomy, University of Colorado, Boulder, CO 80309-0389, USA

⁵Osservatorio Astronomico di Palermo, Piazza del Parlamento 1, 90134 Palermo, Italy

ABSTRACT

We present high-resolution *Chandra* HETGS X-ray spectra of the classical T Tauri star SU Aur. The quiescent X-ray emission is dominated by a 20–40 MK plasma, which contrasts strongly with the cool 3 MK plasma dominating the X-ray emission of the CTTS TW Hya. A large flare occurred during the first half of our 100 ks observation, and we have modelled the emitting plasma both during this flare and during the apparently quiescent periods. During the flare, an extremely high temperature plasma component (at least 60 MK) accounts for the bulk of the emission. There is an indication of the presence of Fe XXVI emission at 1.78 Å, which is maximally formed at 130 MK.

Key words: Stars: X-rays – Stars: activity – Stars: individual: SU Aur – Stars: pre-main-sequence

1. INTRODUCTION

The classical T Tauri stars (CTTS) are pre-main-sequence low-mass objects which continue to accrete from circumstellar disks. Stellar magnetic fields disrupt the inner disk and funnel the accreting matter inward. Because of the star-disk coupling, the CTTS generally rotate more slowly than their diskless relatives, the weak-lined T Tauri stars. This slower rotation may lead to lower levels of coronal activity.

The special nature of CTTS leads to a number of possible observable properties in their X-ray emission, which might distinguish them from WTTS or from active main sequence stars. Differential rotation between star and inner disk could lead to the winding up of field lines, reconnection, and hence large, quasi-periodic flares. Such events may have been observed in the young object YLW 15 (Tsuboi et al. 2000). The star-disk interaction zone is invoked in many different models of jet launching and collimation. The accretion shock on the stellar surface is expected to have a temperature of around 10^6 K (0.1 keV), so cool plasma may dominate the emission measure distribution. Material loaded onto the field lines from the disk could lead to higher density plasma than seen in purely coronal sources, where the particles are evaporated from

the stellar chromosphere. Abundance anomalies, compared to main-sequence dwarfs, might also be expected.

Many of these properties were seen in the spectrum of the nearby (57 pc) CTTS TW Hya. Kastner et al. (2002) observed this star with the *Chandra* HETGS and found that the emission measure distribution was dominated by cool 3 MK plasma, consistent with temperatures expected in an accretion shock. The density sensitive He-like Ne IX triplet at 13.45, 13.55 and 13.7 Å implies $\log n_e = 12.75 \text{ cm}^{-3}$, a high density consistent with a typical CTTS accretion rate of around $10^{-8} M_\odot/\text{yr}$ (Gullbring et al. 2000). The high density and emission measure imply a small emitting volume relative to most coronal sources. The Ne abundance was found to be a factor of 2–3 higher than solar, while Fe and O were deficient. These results were also found by Stelzer & Schmitt (2004), who observed with *XMM-Newton* RGS. They suggested that the abundance anomalies could be due to depletion of grain forming metals in a disk. All these results are consistent with a picture of X-ray emission from accretion shocks caused by dense material falling in from a circumstellar disk.

It is important that spectra of more CTTS are obtained, to ascertain whether this accretion picture is applicable to CTTS as a class. Unfortunately, few CTTS are bright enough to undertake high-resolution spectroscopy with *Chandra* or *XMM-Newton* – TW Hya is itself accessible mainly due to its proximity. SU Aur is one of the X-ray-brightest CTTS and one of the few feasible targets. We present here our *Chandra* HETG spectra of SU Aur and compare them to the TW Hya results and to results for other young stars.

1.1. SU AUR

SU Aur is a relatively massive CTTS, at about $2 M_\odot$ with spectral type G2 III. It has an estimated age of 4–5 Myr and lies in the Taurus-Auriga complex at a distance of 152 pc. The accretion rate is estimated to be around $10^{-8} M_\odot \text{ yr}^{-1}$. *ASCA* observations by Skinner & Walter (1998) showed that the differential emission measure distribution was dominated by hot (~ 20 MK) plasma.

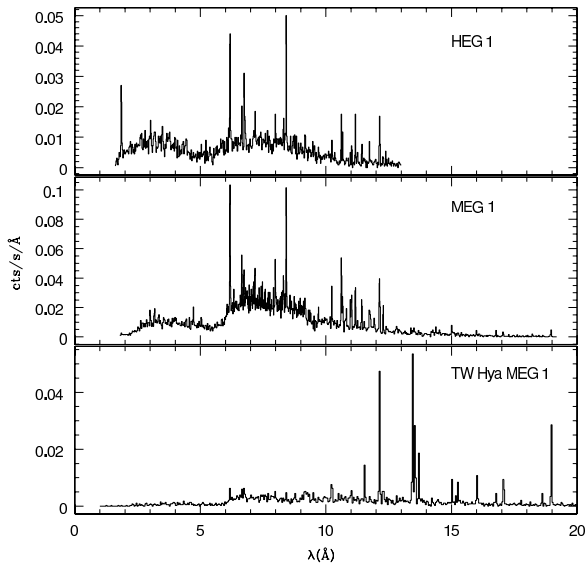


Figure 1. HEG (top) and MEG (middle) spectra for the complete observation of SU Aur. The spectrum of TW Hya is also shown (bottom panel).

2. ANALYSIS

Figure 1 shows the *Chandra* HEG and MEG first-order spectra. Also shown is the MEG 1st order spectrum of TW Hya. The contrast between the spectra of the two stars is immediately clear. The SU Aur spectrum shows the presence of hot continuum emission below 5 Å. Various moderate-temperature lines such as Si XIV (6.2 Å, peak emissivity at 16 MK) and Mg XII (8.4 Å, peak emissivity at 10 MK) are also strong in SU Aur, whilst they are weak or absent for TW Hya. Low-temperature lines such as Ne X at 12.1 Å or O VIII at 16 Å are much stronger in the TW Hya spectrum than for SU Aur.

A further indicator of hot plasma in SU Aur is the presence of Fe XXV emission at 1.85 Å, with a peak emissivity at 60 MK, and Fe XXVI at 1.78 Å, with a peak emissivity at 125 MK. These lines are evidence of a very hot plasma component during the observation.

2.1. FLARING BEHAVIOUR

The MEG 1st order lightcurve (Fig. 3) shows flaring behaviour in the early part of the observation. The large rise here may be caused by at least two separate flares, the second one beginning as the first peaks around $T=13$ ks – producing a ‘shoulder’ in the flare profile at this time. The large flare or flares together radiate approximately 10^{36} erg/s. A further, smaller flare occurred later at around

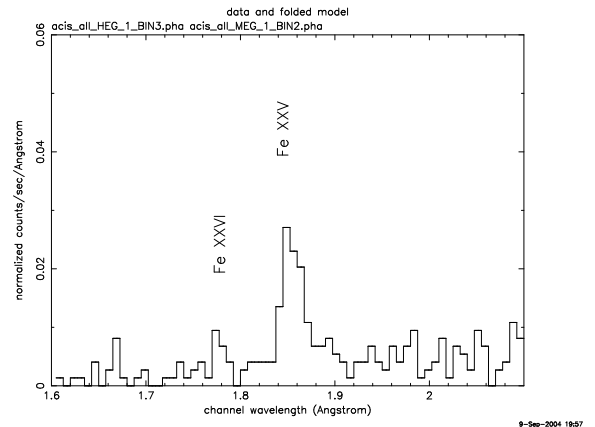


Figure 2. The short-wavelength part of the complete HEG spectrum, showing the Fe XXV line at 1.85 Å and the Fe XXVI line at 1.78 Å.

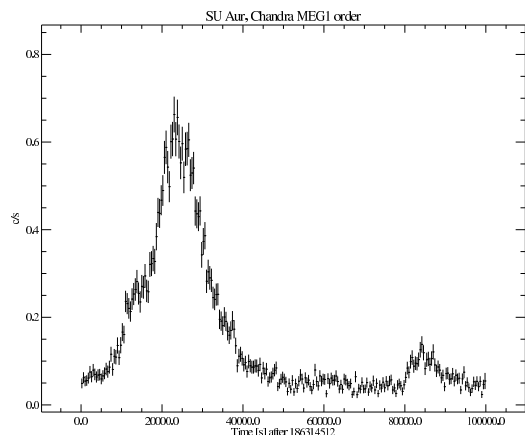


Figure 3. MEG lightcurve. An apparent ‘shoulder’ on the large flare at around 17 ks may indicate that this flare is in fact a composite of at least two successive flare events.

$T=85$ ks. These three components are indicated on the plot, the first one also with an exponential decay. It is therefore sensible to split the analysis between the quiescent and flaring emission, where signal-to-noise constraints allow.

One question which can be posed here is when the Fe XXV, Fe XXVI and short wavelength continuum emission are detected. We obviously expect the bulk of these photons to arrive during the flaring periods, when the plasma component is hottest. In Fig. 4 we show a scatterplot of the arrival times of the various photons in the short-wavelength part of the spectrum. From this figure it can be seen that *no* photons at wavelengths shorter than 1.8 Å arrive during the quiescent periods. The Fe XXV line at 1.85 Å is largely formed during the large flare with some contributions during the later flare and during the

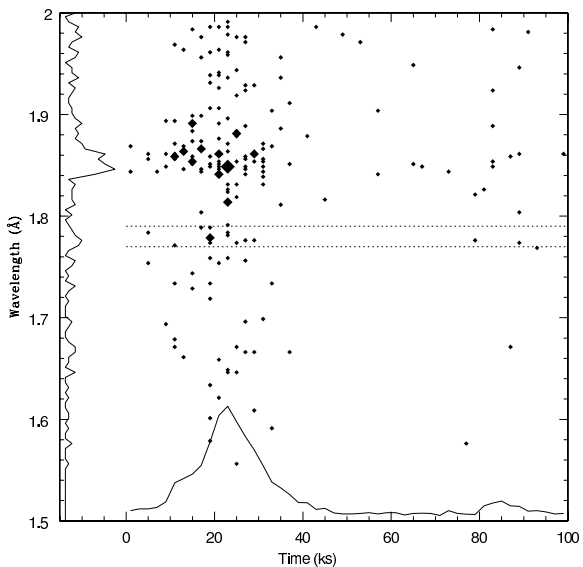


Figure 4. Scatterplot of arrival times (x -axis) of photons against wavelength (y -axis), for the portion of the spectrum below 2 \AA . The spectrum is broken down into 5 ks segments. Larger symbols represent the arrival of 2, 3 or 4 photons in the same 5 ks segment. The lightcurve is plotted on the x -axis, and the spectrum on the y -axis. The dashed lines show the position of the Fe XXVI line.

quiescent periods. The suspected Fe XXVI line is formed only during the flaring periods, with the overwhelming majority of photons arriving during the large early flare.

Models with three temperature components and photoelectric absorption were used to fit the spectra. The background was negligible, and therefore was not subtracted, allowing robust C statistics to be used for the fit. We considered three separate time intervals when fitting models; the period from 5 ks to 22.5 ks, which is dominated by rising flare emission, from 22.5 ks to 50 ks, which is dominated by the flare decay phase, and a quiescent state comprising three intervals, 0–5 ks, 50–80 ks and 90–100 ks. In the case of the quiescent emission, a two-temperature model was found to be sufficient to fit the data. The rise phase is dominated by plasma at around 100 MK and 25 MK. The decay phase is dominated by slightly cooler plasma at around 50 MK and 20 MK. The quiescent plasma is dominated by plasma at around 30–40 MK. These fits further confirmed the strong presence of a very hot (≥ 60 MK) plasma component during the flaring periods, and a hot component (~ 40 MK) which dominates *even during quiescence*. The emission measure

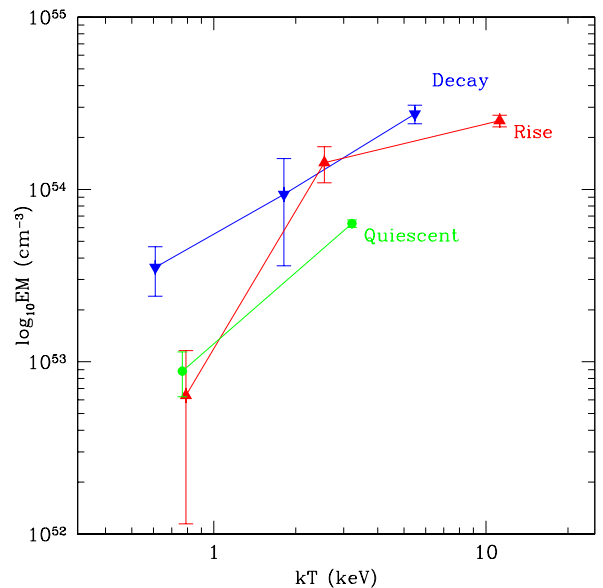


Figure 5. Emission measure and temperature of components of 3-temperature fits to the rising (red, upward-pointing triangles) and decaying (blue, downward-pointing triangles) emission and a 2-temperature fit to the quiescent emission (green, squares).

and temperature of each model component for each fit is shown in Figure 5

A full analysis of the density sensitive He-like triplets has not yet been attempted. Triplets available in the HETGS spectra include S XV at $5\text{--}5.1 \text{ \AA}$, sensitive to densities between $10^{13} - 10^{15} \text{ cm}^{-3}$, Si XIII at $6.6\text{--}6.8 \text{ \AA}$ ($10^{13} - 10^{15} \text{ cm}^{-3}$), Mg XI at $9.2\text{--}9.3 \text{ \AA}$ ($10^{12} - 10^{14} \text{ cm}^{-3}$), and Ne IX at $13.5\text{--}13.7 \text{ \AA}$ ($10^{11} - 10^{13} \text{ cm}^{-3}$). The accretion rate of $10^{-8} M_{\odot} \text{ yr}^{-1}$ suggests a density of around $5 \times 10^{12} \text{ cm}^{-3}$. Unfortunately, the Ne IX and Mg XI triplets, which are sensitive to such low densities, are extremely weak in our spectra. The strongest He-like triplet is Si XIII, shown in Fig. 6. It is clear that the forbidden line here is stronger than the intercombination line, suggesting that the density is less than 10^{13} cm^{-3} .

A preliminary investigation of the abundances of various metals relative to Fe was made by fitting the entire time integrated spectrum. The fitted abundance of Fe was 0.89 solar during quiescence and 1.07 solar during the flare. Abundance ratios relative to Fe were found to be $\text{Mg/Fe}=0.85$, $\text{Si/Fe}=0.89$, $\text{S/Fe}=0.41$, $\text{O/Fe}=0.98$ and $\text{Ne/Fe}=1.08$. There is some evidence that the abundance of oxygen rises during the flaring state ($\text{O/Fe}=0.6$ during quiescence), whilst that of Ne falls ($\text{Ne/Fe}=1.98$ during

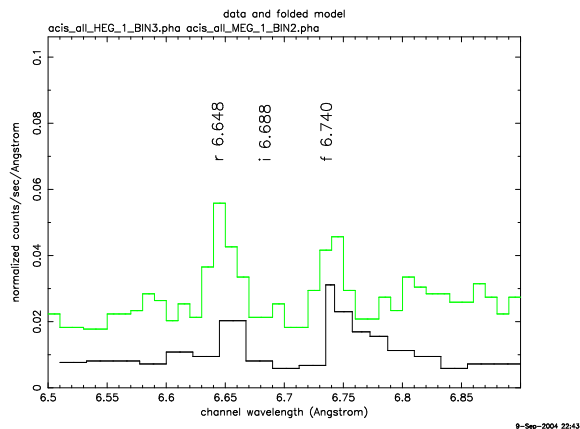


Figure 6. The Si XIII He-like triplet at 6.6–6.8 Å. The MEG spectrum is shown in green (light grey in the black and white version) and the HEG spectrum is in black. The resonance, intercombination and forbidden lines are labelled.

quiescence). A full analysis is necessary before definitive conclusions can be drawn regarding the abundances.

3. CONCLUSIONS

The high-resolution *Chandra* HETGS spectra we present here show clearly the presence of hot (30 MK) plasma in the quiescent emission. This is augmented by the presence of an even hotter component (60+ MK) during the large flares seen in the first half of the observation. The presence of such hot plasma is also indicated by the observation of Fe XXVI at 1.78 Å. Very hot plasma (up to 100 MK) in stellar flares is not unusual in active stars, and has been detected directly in some cases through hard X-ray emission seen with *BeppoSAX* (e.g. Franciosini et al. 2001 on UX Ari, Maggio et al. 2000 on AB Dor and Favata & Schmitt 1999 on Algol). This EM distribution does however make a strong contrast to TW Hya, the only CTTS previously studied at this spectral resolution in the X-ray. Hot (45 MK) plasma is also reported elsewhere in these proceedings for the CTTS RY Tau (Audard et al. 2004). The appearance of the Si XIII forbidden line indicates a density less than 10^{13} cm^{-3} . Although this density constraint is not very stringent, there is no compelling evidence in our preliminary analysis of the SU Aur spectrum for densities as high as those inferred for TW Hya by Kastner et al. (2002). There is evidence from preliminary fitting that the Ne abundance may be high compared to other metals during quiescence, whilst O may have a low abundance (but the Fe abundance appears approximately solar). The Ne and O abundances change towards solar during the flare.

In summary, SU Aur provides at least one counterexample to the properties of TW Hya. It may be that SU

Aur is the unusual object – the sensitivity limits of current high-resolution X-ray spectrometers introduce a strong selection bias – but it would nevertheless be premature to adopt TW Hya as the prototypical classical T Tauri X-ray source at this stage.

ACKNOWLEDGEMENTS

The authors would like to acknowledge support from SAO grants GO3-4015A and G03-4015B, and also from the Swiss NSF (grant 20-66875.01).

REFERENCES

- Audard et al., 2005, These proceedings
- Favata & Schmitt, 1999, A&A 350, 900
- Franciosini et al., 2001, A&A 375, 196
- Gullbring et al., 2000, ApJ 544, 927
- Kastner et al. 2002, ApJ 567, 434
- Maggio et al., 2000, A&A 356, 627
- Skinner & Walter, 1998, ApJ 509, 761
- Stelzer & Schmitt, 2004, A&A 418, 687
- Tsuboi et al. 2000, ApJ 532, 1089